Repulsion and attraction in a couple of cracks

M.-J. Dalbe[a,b], J. Koivisto[c], L. Vanel[b], A. Miksic[c], O. Ramos[b], M. Alava[c], S. Santucci[a]

a. Laboratoire de Physique de l'Ecole Normale Supérieure de Lyon, CNRS and Université de Lyon, France
b. Institut Lumière Matière, UMR5306 Université Lyon 1-CNRS, Université de Lyon, France
c. COMP Center of Excellence, Department of Applied Physics, Aalto University, Finland

Résumé : (16 gras)

Nous avons réalisé une étude expérimentale de l'interaction entre deux fissures colinéaires dans différentes feuilles de polymères soumises à une contrainte uniaxiale à vitesse constante. Nous avons observé différents comportements en fonction de la géométrie des échantillons et du matériau utilisé. Dans certains cas, nous avons observé un régime durant lequel les fissures se repoussent, avec une intensité dépendant de la séparation verticale initiale d. Nous montrons que l'angle θ, caractérisant l'amplitude de la répulsion, dépend fortement du comportement microscopique du matériau. Nous proposons une interprétation de nos résultats expérimentaux basée sur l'observation des formes et tailles des zones d'endommagement en tête de fissure dans les différents matériaux étudiés.

Abstract :

We have performed an experimental study of the interaction of two collinear cracks in different polymer sheets submitted to uniaxial stress at a constant imposed velocity. Depending on the samples geometry and the material used, we could observe that the two cracks interact in different ways. More specifically, we could observe different crack trajectories, with in particular, a repulsive regime, which evolves systematically with the initial vertical crack separation d. We show that the angle θ characterizing the amplitude of the repulsion - and specifically its evolution with d - depends strongly on the microscopic behavior of the material. We provide a physical interpretation of our results, based on the observation of different shape and size of the fracture process zone in the different samples studied. At interaction distances larger than the process zone size, the microscopic shape of the process zone tip controls the amplitude of the crack repulsion, contrary to the macroscopic mechanical behavior of the material [1].

Mots clefs : Fracture mechanics ; Interaction ; Process zone

The propagation of cracks in solids can weaken structures and lead to catastrophic failures. Thus, a better understanding of fracture mechanisms in solids is obviously of crucial importance for a safer design of civil engineering structures. Different studies focused on the propagation of a single crack [2, 3, 4] however, one single crack is rarely at the origin of catastrophic failures, which are more often caused by an array of cracks. The interaction of different cracks leads to kinked trajectories because of the modification of the stress fields around the crack tips. It is observed that cracks often coalesce around a

90° angle, in examples such as drying films [5] or fault dynamics [6, 7]. In particular, many geophysical studies show that two cracks interacting often result in a "hook-shaped" path : the crack ends diverge and then converge towards each other. This shape was observed in nature at different scales : from 25 cm quartz-feldspar veins in granite to 25 km-long oceanic ridges [7]. Some experiments were done to reproduce this pattern in glass [8], PMMA [9], gelatin sheets [10] or in paper sheets [11]. Theoretical studies have tried to explain this truly non-intuitive behavior. First, Melin [12] showed that the collinear crack configuration is unstable. Then, Kachanov [13] noticed that indeed the slightest disturbances in the initial symmetric configuration will give rise to a mixed mode interaction (traction and shear stresses). The fact that the cracks are observed to actually deviate instead of going straight to minimize shear stress led him to suggest that the cracks might actually follow a path that maximizes the energy release rate, instead of the path following the principle of local symmetry [14, 15]. Numerical simulations [16, 17, 18] can only reproduce qualitatively the shapes observed, and most of experimental observations have been performed only on the final post-mortem path (usually obtained in a fast dynamic fracture regime [12, 11]). Finally very few works have studied in details, or even simply ignore the repulsive part of the fracture trajectory [10], and especially the amount of deviation, for which no clear predictions are established. Therefore, we have focused our study on this repulsive regime, when considering the interaction of two collinear cracks in various polymer sheets, submitted to uniaxial stress at a constant slow velocity.

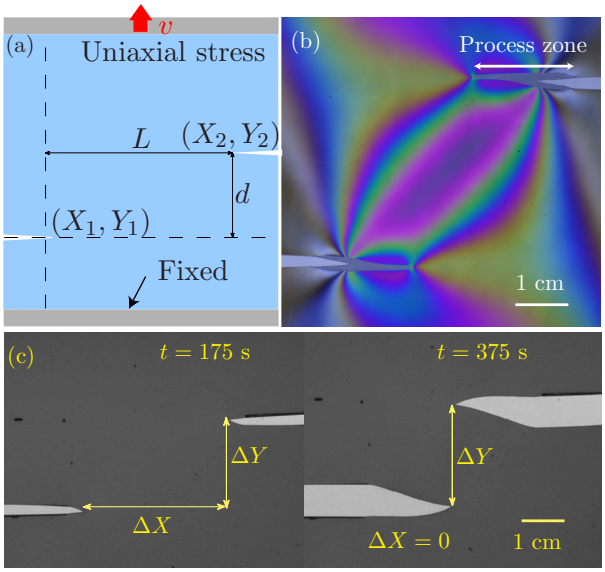

FIGURE 1 – a. Schematic representation of the experimental set-up. A plastic sheet with two initial notches separated by a vertical d and horizontal L distances is submitted to a mode I loading at a constant imposed velocity. We follow the slow interacting growth of the two cracks, with for instance $d = 2$ cm and $L = 4$ cm, in PC samples (close-up in b, in photoelasticity) or PET Mylar® sheets (close-up in c).

The samples are clamped in a tensile testing machine, and pulled from one side at a fixed velocity $v = 0.02$ mm s^{-1} while the other side is fixed (figure 1(a)). We performed experiments with two types of polyester (PET) and polycarbonate (PC) sheets. For PET (resp. PC), The samples are 80×120 mm^2 (resp. 100×120 mm^2), so that when they are clamped, the actual area of study is a square of 80×80 mm^2 (resp. 100×100 mm^2). We prepare two notches, separated vertically by a distance d and vertically by a length L. We vary these two parameters, so that $0 < d < 4$ cm and $1 < L < 8$ cm. During the experiment, we use a standard digital camera to take two pictures per second.

During the experiment, each crack grows quasi-statically. The two cracks interact with each other, and their trajectories do not stay perpendicular to the applied stress. In figure 1(b) and (c), we show typical images from the experiments. The PC sheets display original properties - both mechanical and optical. First, one can observe at the crack tip the development of a macroscopic flame-shaped plastic process zone where the sheet thins[19]. Moreover,under stress, this material becomes birefringent. Thus, we can least observe and characterize qualitatively how the stress field is modified by the presence of another defect, by placing the PC sheets in between two polarizers. In figure 1(b), we observe the specific patterns of the isochromatic fringes (showing the zones of constant principal stress differences) due to the interaction between the cracks and their process zones.

We then study the gray-scale images to extract the trajectory of the crack tip. With image analysis, we are able to detect the crack tips of coordinates (X_1, Y_1) and (X_2, Y_2). We define the variables $\Delta X = X_2 - X_1$ and $\Delta Y = Y_2 - Y_1$ corresponding to the horizontal and vertical distances between the two crack tips (cf figure 1). To characterize the interaction of the cracks, we define $\Delta y = \Delta Y - d - \Delta v$, with Δv the elastic elongation ; $\Delta v \simeq \Delta Y_m - d$, with ΔY_m being the distance between the axes of the two cracks in the deformed state.

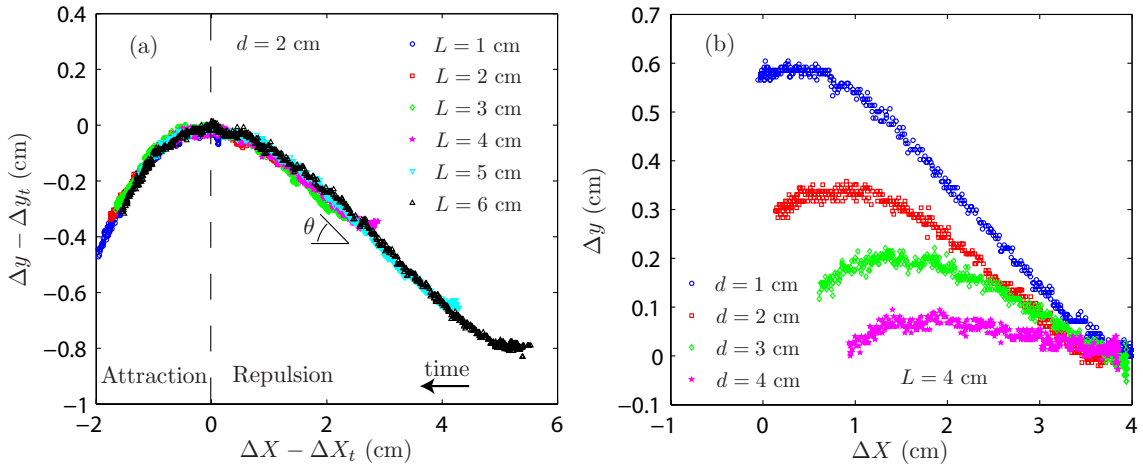

FIGURE 2 – Crack pair trajectories for various experimental conditions obtained with PET Mylar®. We plot in (a) $\Delta y - \Delta y_t$ *vs.* $\Delta X - \Delta X_t$ for $d = 2$ cm, and various L. In (b), we represent $\Delta Y - d$ *vs.* ΔX for $L = 4$ cm, and various d.

We study the crack pair trajectories by analysing the curves Δy vs ΔX for various geometrical configurations. In most cases, we observe that when ΔX decreases (which corresponds to the time increasing), Δy first increases : the two cracks repel each other. Then, Δy reaches a maximum at the point $(\Delta X_t, \Delta y_t)$ and finally decreases : the two cracks attract each other. On figure 2(a), we can observe this typical behavior for $d = 2$ cm and different L, for PET Mylar®. We plot $\Delta y - \Delta y_t$ *vs.* $\Delta X - \Delta X_t$ in order to have the maximum point at $y = 0$ and $x = 0$ so that we can compare quantitatively the trajectories. We observe that they do not depend on L.

In figure 2(b), we plot Δy *vs.* ΔX for a given L and different d for PET Mylar® sheets. The trajectory depends strongly on the initial vertical separation distance d. Moreover, for those experiments (in PET Mylar), the repulsion decreases systematically when d increases : when the cracks are further away, they interact less.

To study in more details the repulsive part of the crack pair trajectories, we define the repulsion angle θ as the maximum slope in the curve Δy *vs.* ΔX. In figure 3, we plot this repulsion angle as a function

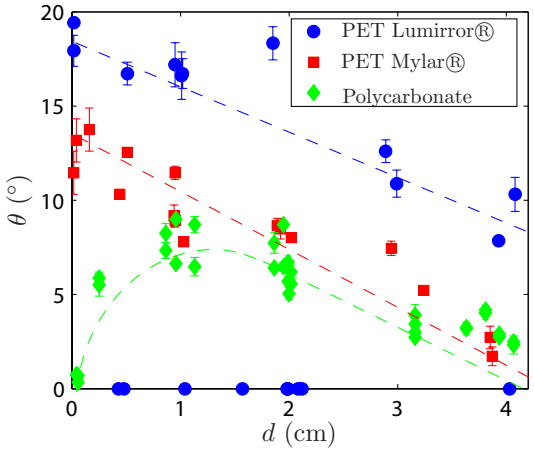

FIGURE 3 – Repulsion angle θ *vs.* d for a given $L = 4$ cm (PET) or $L = 6$ cm (PC), for different types of plastic sheets. Each point represents the estimated slope for one experiment, with its fitting residual as an errorbar. The lines are guide for the eye.

of d for the three studied samples. The case of PET Mylar® is the most straightforward case : each set of parameters gives reproducible experiments and a single value θ, which decreases with d. For the PET Lumirror®, with a given set of parameters we observed two very different behaviors : in one case the two trajectories were straight, with no interaction, giving a zero angle of repulsion. In the other case, the two cracks repelled each other, giving a positive value of θ. This two different behaviors could be the signature of some heterogeneities in the material, which would change the stress field. Indeed, contrary to the PET Mylar®, the PET Lumirror® can be scratched easily, and the samples present some defects on their surfaces. The positive value of θ decreases with d, as observed for PET Mylar®. However the value of θ is systematically larger in this case. This is unexpected since both materials have the same macroscopic mechanical properties (Young's modulus and yield stress), with identical strain-stress curves. Therefore, such results show the limits of theoretical descriptions of the interactions of the cracks based only on linear elastic fracture mechanics. It suggests the importance of nonlinearities in the singular stress field at the crack tips. Indeed, the two PET samples present different microscopic plastic process zones with a sharper tip in

We discuss finally the experimental results on PC sheets, for which a large flame-shaped plastic process zone can be observed at the crack tip. Interestingly, we observe that the evolution of θ is non-monotonic, with a maximum for $d \approx 1$ cm, corresponding roughly to the width of the process zone. Compared to PET samples, the much larger process zone in PC has apparently a screening effect on the repulsive interactions between the two cracks at small d. Interestingly, although the plastic process zone is much larger in PC films, the repulsion angle for large d is the same as in the PET Mylar® samples. We relate this observation to the similar tips of the process zones at "microscopic" scale in the two materials, leading to a similar stress singularity at large enough distance from the process zone.

Références

[1] M.-J. Dalbe, J. Koivisto, L. Vanel, A. Miksic, O. Ramos, M. Alava and S. Santucci, Phys. Rev.Lett. (2015, Accepted)

[2] R. Schapery, Int. J. Fracture **11**, p.141 (1975).

[3] M. Marder and S. Gross, J. Mech. Phys. Solids, **43**, p.1 (1995).

[4] S. Santucci, L. Vanel and S. Ciliberto, Phys. Rev.Lett., **93**, 095505 (2004).

[5] S. Bohn, L. Pauchard and Y. Couder, Phys. Rev. E, **71**, 046214 (2005).

[6] K. Macdonald, J.-C. Sempere and P. Fox, J. Geophys. Res.-Sol. Ea., **89**, p. 6049 (1984).

[7] D. D. Pollard and A. Aydin, J. Geophys. Res.-Sol.Ea., **89**, p. 10017 (1984).

[8] M. Swain and J. Hagan, Eng. Fract. Mech., **10**, 299 (1978).

[9] A. Eremenko, S. Novikov and A. Pogorelov, J. Appl. Mech. Tech. Phy., **20**, 477 (1979).

[10] M. Fender, F. Lechenault and K. Daniels, Phys. Rev. Lett., **105**, 125505 (2010).

[11] P.-P. Cortet, G. Huillard, L. Vanel and S. Ciliberto, J. Stat. Mech.- Theory E., **10**, P10022 (2008).

[12] S. Melin, Int. J. Fracture, **23**, p. 37 (1983).

[13] M. Kachanov (Academic Press INC, 1994), pp. 259–445.

[14] F. Erdogan and G. Sih, J. Fluid Eng., **85**, p. 519 (1963).

[15] B. Cotterell and J. Rice, Int. J. Fracture, **16**, p. 155 (1980).

[16] J.-C. Sempere and K. C. Macdonald, Tectonics, **5**, p. 151 (1986).

[17] H. Chan, Eng. Fract. Mech., **39**, p. 433 (1991).

[18] P. Baud and T. Reuschlé, Geophys. J. Int., **130**, p. 460 (1997).

[19] P.-P. Cortet, S. Santucci, L. Vanel and S. Ciliberto, EPL, **71**, 242 (2005).